

Decontamination of industrial textile wastewater using photocatalysis

José Herney Ramírez-Franco ^a & Hugo Ricardo Zea-Ramírez ^b

^a *Departamento de Ingeniería Química y Ambiental, Universidad Nacional de Colombia, Bogotá, Colombia, jhramirezfra@unal.edu.co*

^b *Departamento de Ingeniería Química y Ambiental, Universidad Nacional de Colombia, Bogotá, Colombia, hrzear@unal.edu.co*

Received: November 21th, 2014 Received in revised form: August 1st, 2015. Accepted: February 25th, 2016.

Abstract

Iron-doped TiO₂ catalysts were prepared by impregnation in order to study their photocatalytic activity in the treatment of wastewater from the textile industry. Characterization of the catalysts before and after reaction was performed using techniques including total surface area measurement, X-Ray diffraction and elemental analysis via X-Ray fluorescence. Varying pH conditions, H₂O₂ concentrations and catalyst quantities were evaluated during the photocatalytic reactions. Fe-TiO₂ catalysts were shown to be highly active in the reduction of chemical oxygen demand (% COD) and % color reduction in the water treated.

Keywords: Fe doped TiO₂, Photocatalysis, Color reduction, COD, Wastewater.

Descontaminación de aguas de desecho de la industria textil usando Fotocatálisis

Resumen

Catalizadores de TiO₂ dopado con hierro se prepararon por impregnación para estudiar su actividad fotocatalítica en el tratamiento de aguas residuales de la industria textil; la caracterización de los catalizadores antes y después de la reacción incluyó área superficie total, difracción de rayos X y análisis elemental por medio de fluorescencia de rayos X. Durante la reacción fotocatalítica se evaluaron varias condiciones de pH, concentración de H₂O₂ y cantidad de catalizador; los catalizadores de Fe-TiO₂ demostraron una alta actividad para la reducción de la Demanda Química de Oxígeno (% DQO) y de % Color de las aguas tratadas.

Palabras clave: TiO₂ dopado con Fe, Fotocatálisis, Reducción de Color, DQO, aguas de desecho.

1. Introduction

Processes used in the textile industry require large amounts of water and generate considerable quantities of contaminated wastewater. The effluents involved usually contain azo-dye colorants along with heavy metals, bleaches and acids which are extremely toxic. Dyes released into the environment can break down into toxic, carcinogenic or mutagenic products [1,2]. The introduction of more stringent regulations by Bogotá's Secretary of the Environment (Resolution 3957/2009) saw the establishment of permitted thresholds for pollution factors including heavy metals, tensoactives, biochemical oxygen demand (BOD), chemical oxygen demand (COD), grease and fat, pH, temperature, suspended solids and Color.

Treatment using chemical methods (e.g., reduction, oxidation) [3,4], physical methods (e.g., adsorption) [5], selective membranes [6], electrochemical processes [6] and biological methods [7,8] have been studied and applied in order to reduce

dye contamination. However, these methods can be site specific, expensive and cumbersome to operate. The efficiency of biological treatment in reducing COD depends heavily on the BOD/COD ratio. The average value of this ratio in the textile industry is 0.35 [9], below the value recommended for total COD removal. The ratio should be increased to a value of not less than 0.6 if acceptable biodegradability in the effluent is to be achieved.

Advanced oxidation processes (AOPs), have attracted interest in the treatment of organic and sometimes inorganic contaminants in wastewater. AOPs are based on physico-chemical processes capable of producing profound changes in the chemical structure of pollutants. The process involves the generation of powerful transient species: the hydroxyl radical (HO[•]) in particular. Such radicals facilitate the oxidation of organic molecules via a reaction mechanism involving hydrogen abstraction or the electrophilic interaction with double bonds forming highly reactive organic radicals (R[•]), which react with oxygen to generate

peroxyl radicals, leading in turn to a chain of oxidative reactions that contribute to the partial or complete degradation of contaminant molecules.

Physical and chemical properties such as photoactivity, chemical stability and nontoxicity have made TiO₂ one of the commonest materials used in photocatalytic applications [10]. TiO₂ is a light sensitive semiconductor that absorbs electromagnetic radiation close to the UV region. This means it is an active photocatalyst capable of producing free radicals that promote partial and complete oxidation [11-14]. Because of its photocatalytic characteristics, TiO₂ has been extensively used in dye removal processes [15,16]. The photo-efficiency of TiO₂ is affected by its wide band-gap energy ($E_g = 3.2$ eV) and the high recombination rate of its photogenerated electron-hole pairs [17]. To overcome these disadvantages, TiO₂ is doped with metals in order to increase its capacity to absorb from the visible portion of the sun's spectrum [18]. Many metal ions, particularly from transition metals, have been used as dopants for TiO₂, and their effects on its performance have been variously reported [10, 19]. Iron has frequently been identified as an appropriate metal ion dopant, because of its electron configuration [20,21].

This paper presents results for the photocatalytic performance of an Fe-TiO₂ catalyst for the decontamination of textile wastewater evaluated for several pH conditions, H₂O₂ concentrations and catalyst quantities, before and after reaction.

2. Materials and Methods

2.1. Wastewater characterization

Several wastewater samples from the textile industry in Bogotá (Colombia) were characterized; the values obtained were compared with the permitted levels established by Resolution 3957/2009 (Table 1). Industrial effluent complies with most of the permitted limit values. However, COD and Color values (identified in boldface) exceeded the standard.

The results reported in Table 1 may be used to calculate the % reduction in COD (76.4%) and Color (97.5%) required to comply with Resolution 3957/2009.

Table 1.
Textile wastewater characterization.

Parameter	Units	Detected	Resolution 3957/2009
Cadmium, Cd	(mg/L)	<0.003	0,02
Nickel, Ni	(mg/L)	<0.07	0.5
Chrome, Cr	(mg/L)	0.06	1,0
Phenols	(mg/L)	<0.07	0,2
Lead, Pb	(mg/L)		0,1
SAAM, tensoactives	(mg/L)	<0.07	10
BOD	(mg/L)	2,686	800
COD	(mg/L)	6,382	1500
Grease and Fat	(mg/L)	69	100
TSS	(mg/L)	255	600
pH		6.42-7.99	9-May
Temperature	(°C)	16-24	<30
Sedimentable solids	(mg/L)	9.0-13	2,0
Color	Pt-Co 1/20 units	2028	50

Source: The authors

2.2. Catalyst synthesis and characterization

The catalysts were prepared using wet impregnation; TiO₂ (Mba8668- Industrial Grade) was impregnated with an aqueous solutions of iron nitrate, Fe(NO₃)₃, (Sigma-Aldrich) of proper concentrations, generating a catalyst with a weight load of 7%. The mixture was kept under constant stirring (250 rpm) for 72 hours at 50°C; the remaining paste was calcined at 450°C with a heating rate of 10°C/min. After calcination, the catalyst was ground and sieved with a mesh size of 200. The catalyst surface areas were evaluated by the Brunauer-Emmett-Teller (BET) method of liquid nitrogen adsorption isotherms at 77 K, using AUTOSORB-1 (QUANTACHROME) equipment. Previous to the N₂ adsorption the catalyst sample was degassed for 20 h at 200°C. Crushed and sieved catalyst samples were characterized by XRD using Ni-filtered Cu-K α radiation in an X-PERT PRO PANALYTICAL diffractometer operating in continuous scan mode between 20 and 80°. JADE Software (MDI, Inc) was used to analyze the collected X-Ray diffraction (XRD) data and compared against the International Centre for Diffraction Data ICDD database. Elemental chemical analysis was performed by means of X-ray fluorescence (XRF) on a ZSX PRIMUS (Rigaku) equipped with a 4kW Rhodium anode.

2.3. Catalyst activity test

Photocatalytic activity was evaluated in a batch reactor made of quartz (250 ml), irradiated by 9 UV-A lamps (wavelength 320 to 400 nm). Reactor and lamps were located inside a temperature-controlled chamber. The reaction volume for all the experiments was 200 ml of reactive solution, adjusted to the pH selected for each experiment. At reaction time equals zero (t=0) the correct amounts of powdered catalyst and hydrogen peroxide, defined during experimental design, were added to the reaction volume, light sources being switched on simultaneously. All experiments were carried out at room temperature. COD and Color changes were determined by spectrophotometric methods, in compliance with the US EPA Standard Methods 5220-D and Standard Methods 2120 C, respectively [22].

3. Results and Discussion

3.1. Catalyst characterization

The XRD patterns of the fresh catalyst (after calcination) and following reaction are shown in Fig. 1 (profiles a and b, respectively). The XRD profiles revealed a high crystallinity with a predominantly rutile phase (characteristic peaks at 2 θ angles equal to: 27.6°, 37.2°, 54.46°). In addition, weak and broad peaks at 2 θ angles 56.7° and 41.2° indicated that the iron was present as small well dispersed magnetite crystals (Fe₃O₄). No major change was observed by XRD in the catalyst after it had been used several times in the reaction. This structural stability is related to the low catalyst deactivation apparent during the deactivation tests.

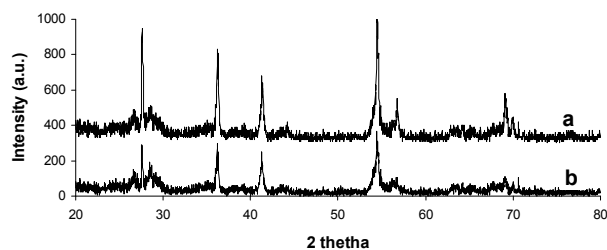


Figure 1. XRD profiles of catalyst (a) fresh and (b) after reaction.
Source: The authors.

Table 2.

Experimental conditions of COD reduction experiments and % COD reduction.

Test No	pH	Fe-TiO ₂ g/L	H ₂ O ₂ × 10 ⁻³ [M]	% COD Reduction
E1	3	1.0	3	95
E2	3	1.0	6	95
E3	3	1.0	9	95
E4	3	1.5	3	89
E5	3	2.0	3	88
E6	5	1.0	3	63
E7	5	1.0	6	74
E8	5	1.0	9	77
E9	5	1.5	3	66
E10	5	2.0	3	59
E11	5	1.5	6	69
E12	5	1.5	9	79
E13	3	1.5	9	97
E14	5	2.0	6	69
E15	5	2.0	9	72
E16	3	1.5	6	95
E17	3	2.0	9	92
E18	3	2.0	6	89
E19	5	2.0	3	59

Source: The authors

The N₂ adsorption isotherm of the fresh catalyst at 77 K and after reaction shows the typical behavior of a Type III isotherm with a characteristic Type H4 hysteresis, common in low surface area materials. BET surface area values calculated for the fresh (13.22 m²/g) and after reaction (13.35 m²/g) catalyst show no change in surface area of the catalyst as a result of continuous exposure to reaction conditions. X-ray fluorescence (XRF) results of the synthesized catalyst confirms the expected iron loading, close to 7.17% in weight.

3.2. Catalyst activity

Table 2 summarizes experimental conditions for all the activity experiments performed and the % COD reduction achieved. These experiments cover a wide spectrum of operation conditions achieved by varying the amount of catalyst added to the reaction solution, initial pH, and H₂O₂ dosage. The concentration values used are based on previous research [23].

The % COD reduction reported in Table 2 was measured after 180 minutes of reaction. The lowest % COD reduction achieved was 59% at pH 5, using 2.0 g/L of Fe-TiO₂ and 3 mM H₂O₂. The highest % COD reduction (97%) was obtained at pH 3, using 1.5 g/L of Fe-TiO₂ and 9 mM H₂O₂.

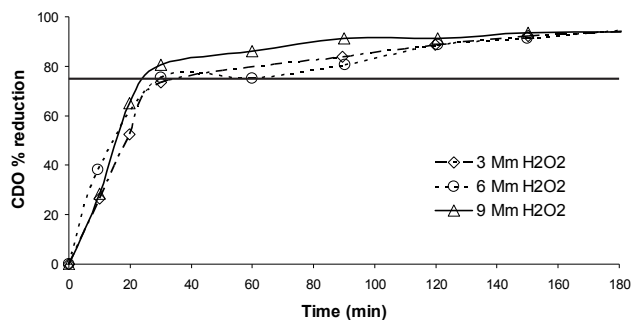
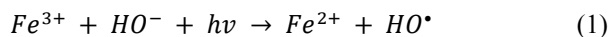


Figure 2. H₂O₂ effect on % COD reduction, C_{catalyst} = 1 g/L, pH = 3.
Source: The authors.

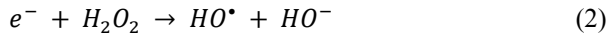
Most of the experiments run at pH 3 (6 out of 9) saw % COD reduction above 90% and only 3 were below 90%. But even these were above 88%. By contrast, in all of the experiments run at pH 5 reduction was below the 77% COD required to comply with Resolution 3957/2009.

Figs. 2 to 4 present the profiles of the reactions corresponding to pH 3. As described previously all the reactions performed at pH 3 had reduction values above 77%, enough to comply with Resolution 3957/2009. Fig. 2 shows the % COD reduction for the experiment using 1 g/L of Fe-TiO₂ for different H₂O₂ concentrations. There is no significant difference in the profiles of each of the H₂O₂ concentrations, all of which rapidly reduced the % COD in the first 40 minutes of the experiment, reaching the reduction goal (77%, represented in the figure by the continuous horizontal line) in about 35 minutes; after 40 minutes the three profiles reached COD reduction values above 90%, while after 140 minutes a plateau of around 96% COD reduction was reached.

During experiments performed with different dosage of H₂O₂ in the reaction solutions (see Fig. 2), the Fe-TiO₂ photocatalytic activity indicated a significant increase in the formation of the OH radical, which was certainly caused by iron oxidation in a photo-Fenton reaction, as follows (1):



By contrast, in the case of the % COD reduction profiles for the experiments with 1.5 g/L of Fe-TiO₂, there was a clear difference between the initial % COD reduction rate of the 3 mM of H₂O₂ that reached 77% reduction in just under 20 minutes before it slowed down dramatically, reaching only 89% of reduction at 180 minutes and finishing below the % COD reduction achieved by the 6 and 9 mM of the H₂O₂ experiments (Fig. 3). The 6 and 9 mM of H₂O₂ % COD reduction profiles followed an almost identical tendency, starting slowly compared to the experiment run at 3 mM of H₂O₂, which reached 77% of COD reduction after 90 minutes, attaining 96 and 97% after 180 minutes, respectively. H₂O₂ can play a dual function: as a strong oxidant itself and as an electron scavenger; proper H₂O₂ concentration has been found to enhance the degradation rate of compounds, as a result of greater efficiency in the generation of hydroxyl radicals and the inhibition of electron-hole pair recombination, according to the following equation (2):



Several experiments previously performed within our research group and reported elsewhere [23], coincide in the identification of suitable H_2O_2 concentrations. At higher concentrations, scavenging of HO^\bullet radicals will occur, as described by the following reaction (3):

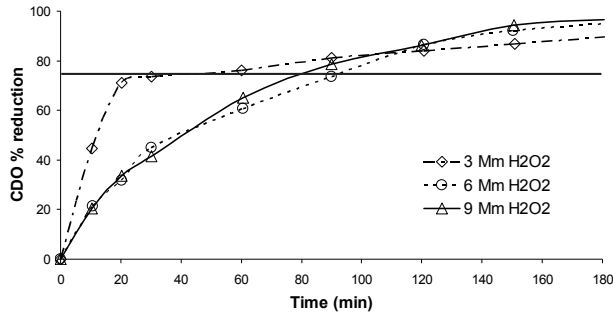
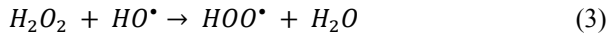


Figure 3. H_2O_2 effects on % COD reduction, $C_{catalyst} = 1.5\text{ g/L}$, $\text{pH} = 3$. Source: The authors.

Fig. 4 shows the % COD reduction for the experiment using 2 g/L of $Fe\text{-}TiO_2$ for different amounts of H_2O_2 . Initially there was a difference in the rate of COD reduction, the 3 and 9 mM H_2O_2 concentrations being, respectively, the fastest and slowest. As the reaction time went beyond 100 minutes the difference grew smaller and after 180 minutes all achieved COD reductions above 90%.

The results for % COD reduction of the 3 different catalyst amounts with the fixed dosage of H_2O_2 indicated an apparent detrimental effect as the amount of catalyst increased: at 1 g/L of catalyst, 77% COD reduction was reached before 40 minutes, independently of the H_2O_2 dosage used. There was, furthermore, little difference between the rate of reduction, all of which reached % COD reduction above 90% after 160 minutes. In the experiments using 1.5 g/L and 2 g/L of catalyst (with the exception of the one using 3 mM H_2O_2 dosages with 1.5 g/L), all the % COD reduction profiles underperformed compared to the results obtained for the 1 g/L experiments. A clear trend has been identified in the literature in terms of the effects of homogeneous iron concentration in Fenton processes, suggesting that an excess of homogenous iron in the reaction consumes free radicals and organically generated free radicals (HO^\bullet) via parallel reaction, reducing the possibility that the radical will continue with the

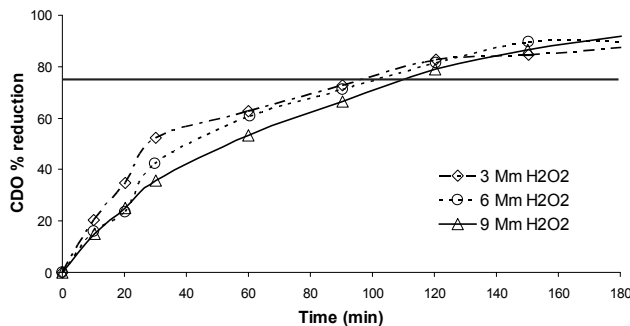


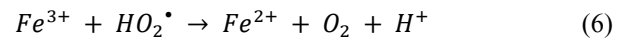
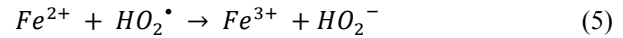
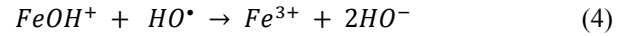
Figure 4. H_2O_2 effect on % COD reduction, $C_{catalyst} = 2\text{ g/L}$, $\text{pH} = 3$. Source: The authors.

Table 3. Experimental conditions of Color reduction experiments and % COD reduction

Test No	pH	Fe-TiO ₂ g/L	H ₂ O ₂ x10 ⁻³ [M]	% Color Reduction
EC1	3	1.0	3	97
EC2	3	1.0	6	98
EC3	3	1.0	9	98
EC4	3	1.5	3	96
EC5	3	2.0	3	90
EC6	3	1.5	9	97
EC7	3	1.5	6	95
EC8	3	2	9	94
EC9	3	2	6	92

Source: The authors

oxidation (degradation) of the contaminant molecule. Some of the proposed chemical reactions through which homogeneous iron reacts are shown:



These % COD reduction experiments allow us to conclude that pH 3 and lower quantities of catalyst in the reaction are beneficial for the oxidation process.

Table 3 summarizes the conditions of the the Color reduction experiments performed and the % Color reduction obtained.

The % Color reduction reported in Table 3 was measured after 180 minutes of reaction. The lowest % Color reduction achieved was 90% using 2.0 g/L of $Fe\text{-}TiO_2$ with a concentration of 3 mM H_2O_2 and the highest (97%) using 1 g/L of $Fe\text{-}TiO_2$ and a dosage of 6 and 9 mM H_2O_2 . It is important to highlighted that the 3 mM H_2O_2 with 1g/L of $Fe\text{-}TiO_2$ also achieved a high % Color reduction (97%), virtually the same value as with the 6 and 9 mM H_2O_2 dosage. The 1 g/L TiO_2 experiments outperformed all the % Color reduction experiments, independently of H_2O_2 dosage.

Figs. 5, 6 and 7 present the profiles of the reactions corresponding to catalyst amounts 1, 1.5 and 2 g/L. In the case of the 1 g/L experiments, the reaction profile followed the same trend as for the three H_2O_2 dosages, reaching 97.5% of Color reduction after 160 minutes. For the experiment run using 1.5 g/L the % Color reduction rate showed a small difference, as a function of H_2O_2 dosage: the 3 mM H_2O_2 dose being slightly more active than the 6 and 9 mM H_2O_2 doses. This small difference disappeared after 160 minutes when all three experiments achieved a % Color reduction above 90%, but barely reached the target Color reduction of 97%. None of the experiments run at 2 g/L $Fe\text{-}TiO_2$ reached the target Color reduction value.

Most of the experimental data collected in the photocatalytic tests showed an initial fast reduction of COD (between 0 and 20 minutes). After the initial fast reduction the degradation rate reduced considerably. Experiments performed in our research group for the same reaction, using several types of catalyst, have shown similar behavior [23], which has also been reported by independent studies [24] that

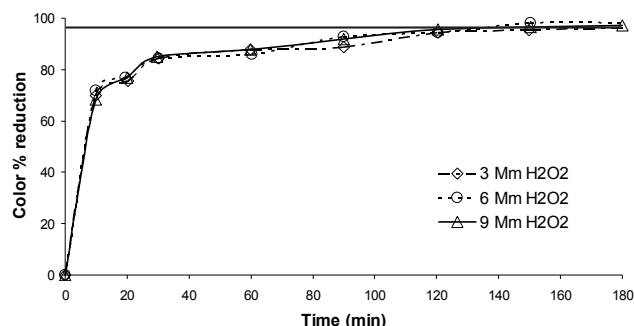


Figure 5. H₂O₂ effect on % Color reduction, C_{catalyst} = 1g/L, pH = 3. Source: The authors.

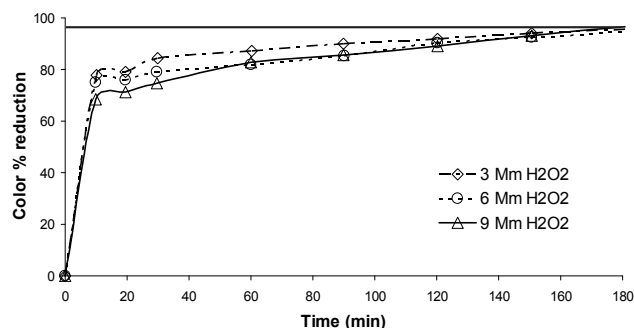


Figure 6. H₂O₂ effect on % Color reduction, C_{catalyst} = 1.5g/L, pH = 3. Source: The authors.

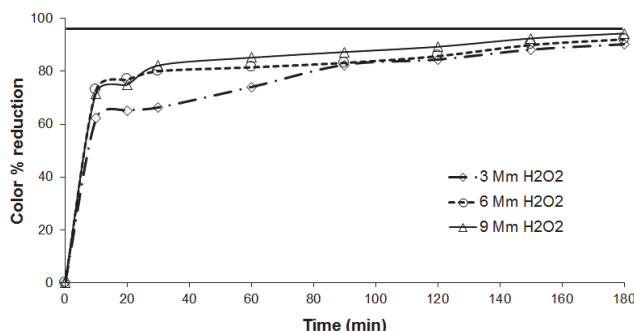


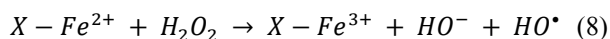
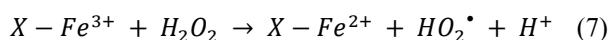
Figure 7. H₂O₂ effect on % Color reduction, C_{catalyst} = 1.5g/L, pH = 3. Source: The authors.

have related this characteristic behavior to a two stage degradation mechanism, typical in Fenton processes. In this mechanism ferrous ions react rapidly with peroxide to form hydroxyl radicals and ferric ions. The hydroxyl radicals formed degrade the contaminant molecule very actively. These ferric ions might react with peroxide to generate hydroperoxyl radicals and ferrous ions.

Textile industry dyes normally consist of molecules formed by benzene and naphthalene rings bonded by an azo linkage (N=N), all of which exhibit different absorbance peaks. The chromophore containing the azo linkage has absorption in the visible region, while the benzene and naphthalene rings absorb in the UV region. Indeed, the disappearance of the absorbance signal in the visible range corresponds to an almost complete decolorization (breakdown of the chromophore group). The rupture of the

bond between the benzene and naphthalene rings generate additional contaminant molecules that must be mineralized, thus increasing the COD values the catalyst must reduce.

The mechanism of the homogeneous Fenton H₂O₂ oxidation decomposition process is not well established. Many oxidizing species have been suggested as being involved, in addition to the HO radicals. Some of the literature [25] has proposed an initial and rapid adsorption of the peroxide molecule on the catalytic specie (Fe³⁺). However, other papers have suggested a different initial reaction step in which the organic molecule is the one adsorbed on the catalytic specie [26]. Nevertheless, the involvement of the following steps has been suggested in most of the works found in the literature, which correspond to the Fe³⁺ reduction generating moderate oxidative HO₂ radicals, followed by Fe³⁺ regeneration with formation of the hydroxyl radicals:



where X represents the surface of the catalyst. However, it should be remarked that the radicals can also be generated on the surface of the solid catalytic material, so that they are actually “caged” in the solid structure, subsequently reacting with the adsorbed reagent(s) without generating radicals. Obviously, in addition to the steps indicated here, many other radical reactions occur, including those involving the reaction intermediates.

TiO₂ crystallinity can greatly influence the photocatalytic activity, which is widely believed to be phase-dependent. The XRD result shows a well define rutile phase before and after reaction, eliminating any possible variance in the photocatalytic activity originated by differences in the crystal phases. Furthermore, the XRD profiles indicate that superficial iron species are present as magnetite crystals and that there is no formation of any iron-titanium solid solution. Generally the effect of the addition of a dopant element to TiO₂ is to facilitate the mechanism by which the conduction band electrons (e⁻) and the valence band holes are generated at the surface by light energy values equaling or exceeding the band gap energy [27]. These holes may react with either the surface hydroxyl ions or with water to produce hydroxyl radicals (OH[•]). The electrons react with adsorbed molecular oxygen, to yield superoxide anion radicals [28] that act as oxidizing agents, thus providing an additional source of the hydroxyl radicals. These hydroxyl radicals are strong oxidants that can react with the dye molecules, leading to their destruction. These types of behavior have also been reported for the treatment of chemical industry wastewater using a solar photoreactor and Titanium Dioxide (Degussa P-25) [29].

4. Conclusions

The photocatalytic performance of an Fe-TiO₂ catalyst for the decontamination of textile wastewater has been evaluated in order to achieve compliance with Resolution 3957/2009 emitted by the Bogotá Secretary of the Environment. Catalyst characterization shows a low surface area non-iron-titanium solid solution of 7.17% Fe₃O₄ (magnetite) supported on a well-

defined rutile phase. Before and after reaction, characterization reveals no major changes in the crystal structure, surface area or catalyst composition as a result of catalyst exposure to reaction conditions. Characterization of wastewater from the textile industry showed deficiencies in the treatment of the COD and Color parameters. An Fe-TiO₂ catalyst prepared by impregnation showed a high % COD and % Color reduction - high enough, indeed, to comply with Resolution 3957/2009

Acknowledgements

The authors would like to thank Diana Varela for the experimental work on which this paper is based and the manager and technicians of the Electrochemistry and Catalysis Laboratory of the Chemical Engineering Department at the National University of Colombia.

References

- [1] Zaharia, C. and Suteu, D., Optimization study of orange 16 dye sorption from aqueous systems using sawdust wastes. *Chemical Bulletin of Politehnica University of Timisoara*, 56(70), pp. 24-28, 2011.
- [2] Sharma, S., et al., Toxicity assessment of textile dye wastewater using swiss albino rats. *Australasian Journal of Ecotoxicology*, 13, pp. 81-85, 2007.
- [3] Brown, G. and JR., D., Photo reduction of methylorange sensitized by colloidal titanium dioxide. *J Chem Soc Faraday Trans*, 80, pp. 1631-1643, 1984. DOI: 10.1039/F19848001631.
- [4] Slokar, Y. and A., Le Marechal, Methods of decoloration of textile wastewater. *Dyes Pigments*, 37, pp. 335-356, 1998. DOI: 10.1016/S0143-7.
- [5] DeJohn, P.B. and Hutchins, R.A., Treatment of dye wastes with granular activated carbon. *Journal Textile Chemist and Colorist*, 8, pp. 34-38, 1976.
- [6] Suarez-Parra, R., et al., Visible light-induced degradation of blue textile azo dye on TiO₂/CdO-ZnO coupled nanoporous films. *Solar Energy Materials and Solar Cells*, 76(2), pp. 189-199, 2003. DOI: 10.1016/S0927-0248(02)00346-X.
- [7] Kalyushnyi, S. and Sklyar, V., Biomineralisation of azo dyes and their breakdown products in anaerobic-aerobic hybrid and UASB reactors. *Water Sci. Technol.*, 41, pp. 23-30, 2000.
- [8] Yoo, E., Libra, J. and Wiesmann, U., Reduction of azo dyes by desulfobivrio desulfuricans. *Water Science & Technology*, 41(12), pp. 15-22, 2000.
- [9] Andreozzi, R., et al., Advanced Oxidation Processes (AOP) for water purification and recovery. *Catalysis Today*, 53(1), pp. 51-59, 1999. DOI: 10.1016/S0920-5861(99)00102-9.
- [10] Maji, S.K., et al., Effective photocatalytic degradation of organic pollutant by ZnS nanocrystals synthesized via thermal decomposition of single-source precursor. *Polyhedron*, 30(15), pp. 2493-2498, 2011. DOI: 10.1016/j.poly.2011.06.029.
- [11] Davidson, A. and Che, M., Temperature-induced diffusion of probe vanadium (IV) ions into the matrix of titanium dioxide as investigated by ESR techniques. *The Journal of Physical Chemistry*, 96(24), pp. 9909-9915, 2002. DOI: 10.1021/j100203a061.
- [12] Fujishima, A., Rao, T.N. and Tryk, D.A., Titanium dioxide photocatalysis. *Journal of Photochemistry and Photobiology C: Photochemistry Reviews*, 1(1), pp. 1-21, 2000. DOI: 10.1016/S1389-5567(00)00002-2.
- [13] Fujishima, A. and Zhang, X., Titanium dioxide photocatalysis: present situation and future approaches. *Comptes Rendus Chimie*, 9(5-6), pp. 750-760, 2006. DOI: 10.1016/j.crci.2005.02.055.
- [14] Noh, J.H., et al., Microwave dielectric properties of nanocrystalline TiO₂ prepared using spark plasma sintering. *Journal of the European Ceramic Society*, 27(8-9), pp. 2937-2940, 2007. DOI: 10.1016/j.jeurceramsoc.2006.11.018.
- [15] Mu, Y., et al., TiO₂-mediated photocatalytic degradation of Orange II with the presence of Mn²⁺ in solution. *Journal of Photochemistry and Photobiology A: Chemistry*, 163(3), pp. 311-316, 2004. DOI: 10.1016/j.jphotochem.2003.08.002.
- [16] Rao, K.V.S., Lavédrine, B. and Boule, P., Influence of metallic species on TiO₂ for the photocatalytic degradation of dyes and dye intermediates. *Journal of Photochemistry and Photobiology A: Chemistry*, 154(2-3), pp. 189-193, 2003. DOI: 10.1016/S1010-6030(02)00299-X.
- [17] Franco, A., et al., Photocatalytic decolorization of methylene blue in the presence of TiO₂/ZnS nanocomposites. *J Hazard Mater*, 161(1), pp. 545-550, 2009. DOI: 10.1016/j.jhazmat.2008.03.133.
- [18] Kiwi, J. and Morrison, C., Heterogeneous photocatalysis. Dynamics of charge transfer in lithium-doped anatase-based catalyst powders with enhanced water photocleavage under ultraviolet irradiation. *The Journal of Physical Chemistry*, 88(25), pp. 6146-6152, 2002. DOI: 10.1021/j150669a018.
- [19] Luo, Z. and Q.-H. Gao, Decrease in the photoactivity of TiO₂ pigment on doping with transition metals. *Journal of Photochemistry and Photobiology A: Chemistry*, 63(3), pp. 367-375, 1992. DOI: 10.1016/1010-6030(92)85202-6.
- [20] Adán, C., et al., Structure and activity of nanosized iron-doped anatase TiO₂ catalysts for phenol photocatalytic degradation. *Applied Catalysis B: Environmental*, 72(1-2), pp. 11-17, 2007. DOI: 10.1016/j.apcatb.2006.09.018.
- [21] Herrmann, J.-M., Heterogeneous photocatalysis: Fundamentals and applications to the removal of various types of aqueous pollutants. *Catalysis Today*, 53(1), pp. 115-129, 1999. DOI: 10.1016/S0920-5861(99)00107-8.
- [22] APHA, A.W., Standard methods for the Examination of water and water and wastewater. 16 Ed, 1995.
- [23] Ramirez, J.H., Costa, C.A. and Madeira, L.M., Experimental design to optimize the degradation of the synthetic dye Orange II using Fenton's reagent. *Catalysis Today*, 107(1), pp. 68-76, 2005. DOI: 10.1016/j.cattod.2005.07.060.
- [24] Malik, P.K. and Saha, S.K., Oxidation of direct dyes with hydrogen peroxide using ferrous ion as catalyst. *Separation and Purification Technology*, 31(3), pp. 241-250, 2003. DOI: 10.1016/S1383-5866(02)00200-9.
- [25] Dantas, T.L.P., et al., Treatment of textile wastewater by heterogeneous Fenton process using a new composite Fe₂O₃/carbon. *Chemical Engineering Journal*, 118(1), pp. 77-82, 2006. DOI: 10.1016/j.cej.2006.01.016.
- [26] Feng, J., et al., A novel laponite clay-based Fe nanocomposite and its photo-catalytic activity in photo-assisted degradation of Orange II. *Chemical Engineering Science*, 58(3), pp. 679-685, 2003. DOI: 10.1016/S0009-2509(02)00595-X.
- [27] Han, T., Wu, C. and Chien-Te, H., Hydrothermal synthesis and visible light photocatalysis of metal-doped titania nanoparticles. *Journal of Vacuum Science*, 25(2), pp. 430-435, 2009. DOI: 10.1116/1.2714959.
- [28] Ya-Fang, T., et al., Preparation of Fe-doped TiO₂ nanotube arrays and their photocatalytic activities under visible light. *Materials Research Bulletin*, 45(2), pp. 224-229, 2010. DOI: 10.1016/j.materresbull.2009.08.020.
- [29] Restrepo, G., et al., Evaluation of photocatalytic treatment of industrial wastewater using solar energy. *DYNA*, 75(155), pp. 145-153, 2008.

H. Zea, received his BSc. Eng. in Chemical Engineering, in 1997, from the Fundación Universidad de America, Bogotá, Colombia, his MSc. in Chemical Engineering in 2000, from the Universidad Nacional de Colombia, Bogotá, Colombia and his PhD. in Chemical Engineering in 2004, from the University of New Mexico, Albuquerque, USA. Between 2005 and 2007 he worked in alternative energy research, followed by a Postdoctoral appointment from mid-2007 to 2008. Since 2008 he has been associate professor at the Chemical and Environmental Engineering Department at the Universidad Nacional de Colombia, Bogotá, Colombia. His research interests include materials, chemical reactions, separation processes and environmental remediation. ORCID: 0000-0002-6801-1879.

J.H. Ramirez, received his BSc. Eng. in Chemical Engineering in 1998, from the Universidad Nacional de Colombia, Manizales, Colombia, his MSc. in Chemical Engineering in 2003, from the Universidade Sao Paulo, Brazil and his PhD. in Chemical Engineering in 2008, from The Universidade do Porto, Portugal. Since 2008 he has been associate professor at the Chemical and Environmental Engineering Department at Universidad Nacional de Colombia, Bogotá, Colombia. His research interests include materials, chemical reactions, environmental catalysis and environmental remediation. ORCID: 0000-0003-1766-1174.